AGU PUBLICATIONS

Geophysical Research Letters

RESEARCH LETTER
10.1002/2015GL066227

Key Points:
- We explore the slab anisotropy in the subducting Philippine Sea plate
- The fast axis is found to be N65°E with splitting time of 0.13 to 0.45 s
- Slab anisotropy is found to be similar to mantle wedge but weaker than upper mantle effects

Supporting Information:
- Figures S1–S9

Correspondence to:
K. H. Chen,
katepili@gmail.com

Citation:
Chen, K. H., Y.-L. Tseng, T. Furumura, and B. L. N. Kennett (2015), Anisotropy in the subducting slab: Observations from Philippine Sea plate events in Taiwan, *Geophys. Res. Lett.*, *42*, doi:10.1002/2015GL066227.

Received 16 SEP 2015
Accepted 16 NOV 2015
Accepted article online 24 NOV 2015

Anisotropy in the subducting slab: Observations from Philippine Sea plate events in Taiwan

Kate Huihsuan Chen[1], Yu-Lung Tseng[2], Takashi Furumura[3], and Brian L. N. Kennett[4]

[1]Department of Earth Sciences, National Taiwan Normal University, Taipei, Taiwan, [2]Department of Geosciences, National Taiwan University, Taipei, Taiwan, [3]Earthquake Research Institute, University of Tokyo, Tokyo, Japan, [4]Research School of Earth Sciences, Australian National University, Canberra, ACT, Australia

Abstract In the southernmost Ryukyu subduction zone, slab-guiding behavior from intermediate-depth earthquakes is well documented with a low-frequency (<2 Hz) first *P* arrival followed by sustained high-frequency (3–10 Hz) wave trains. Such waves developed by propagating along a long path within the slab are expected to have high sensitivity to anisotropy within the slab. We determine shear wave splitting parameters from 178 intraplate events that are deeper than 100 km. The possible slab-anisotropy-associated polarization pattern shows the fast direction at N65°E and delay time of 0.13–0.45 s. This is stronger than the previously documented crust effect (<0.1 s), similar to the mantle wedge effect (0.28 s in average), but weaker than the upper mantle effect (1.3 s in average) in Taiwan. The fast axis reflects the fossil spreading direction of Philippine Sea plate with minor clockwise rotation due to the collision to Eurasian plate.

1. Introduction

Fossil fabric within the oceanic lithosphere and faulting/hydration in the upper layer of the slab are expected to play an important role in the anisotropic signature of a subducted slab [*Forsyth*, 1975; *Nishimura and Forsyth*, 1989; *Faccenda et al.*, 2008; *Healy et al.*, 2009; *Song and Kim*, 2012; *Long*, 2013]. Over the past few decades, despite advances in characterizing anisotropy using shear wave splitting method, the character of slab anisotropy remains debatable. This is likely to be due to the poor depth resolution of shear wave splitting measurements [*Long and Silver*, 2009] and difficulty in isolating the effect of slab anisotropy from other parts of the subduction system (mantle wedge, subslab mantle, and overriding plate). Such issues are linked to the relatively short travel distance through the slab.

Seismic waves traveling up the subducted plate to fore-arc stations with long path lengths in the slab itself provide new insight into the better understanding of seismic anisotropy within the subducted plate. Such seismic waves have been documented as slab-guided waves in the Pacific plate and Philippine Sea plate subducting beneath Japan, where amplified and long-lasting high-frequency (>2 Hz) energy can be associated with scattering by fine-scale heterogeneity in the slab [*Furumura and Kennett*, 2005; *Furumura and Kennett*, 2008]. Polarization analysis of the low-frequency ($f < 2$ Hz) *P* wave onset reveals significant amount of energy on vertical and radial components but not the transverse component. This polarization indicates that the most of the seismic waves propagating in the slab travel along the great circle path. Similar slab-guided behavior from intermediate-depth intraplate earthquakes in Taiwan has been documented by *Chen et al.* [2013], which motivates this study to exploit the paths for slab anisotropy using shear wave splitting measurements.

The northwest moving Philippine Sea plate (PSP) collides with Eurasian plate (EP) in the immediate neighborhood of Taiwan, resulting in orthogonal opposed subduction. In northeast Taiwan, the PSP subducts underneath the rifted EP margin along the Ryukyu trench, whereas in southwest Taiwan the EP subducts beneath PSP along the Malina trench. As shown in Figure 1, the Ryukyu subduction zone terminates against northeast Taiwan, providing a unique condition for nearly vertical propagation from intermediate-depth earthquakes, and good coverage of raypaths in the subduction zone system. Compared with earlier studies for shear wave splitting exploiting *SKS*/*SKKS* phases, local *S* waves with longer paths along the slab can produce effective shear wave splitting parameters for slab anisotropy.

2. Shear Wave Splitting Measurements on Subduction Zone Guided Waves

We use BATS (Broadband Array in Taiwan for Seismology) waveform data for $M \geqq 4$ earthquakes that occurred at depths deeper than 100 km in southernmost Ryukyu subduction zone in the period from 1996 to 2012 and

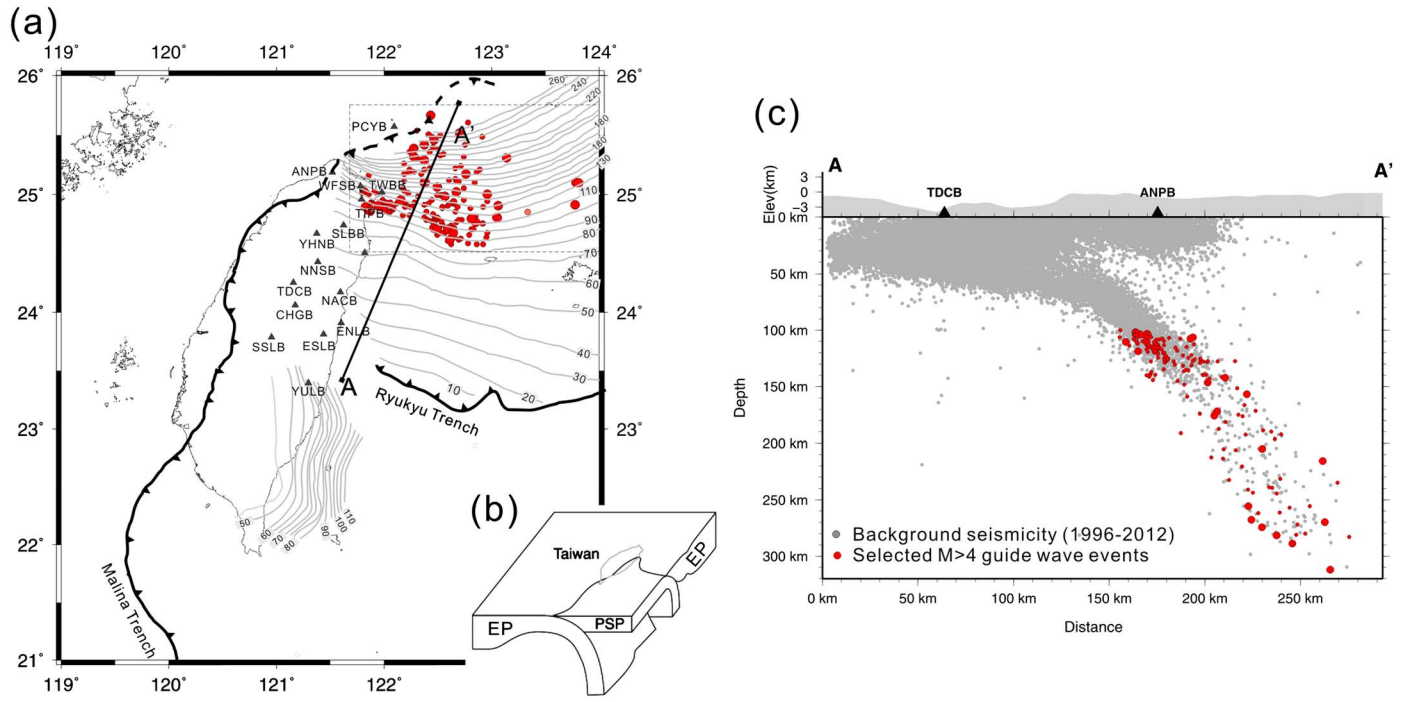

Figure 1. (a) The distribution of BATS broadband stations (black triangles) and $M \geqq 4$ earthquakes from 1996 to 2012 (red circles) used in this study. Grey contours indicate the isodepth of the PSP and EP Moho [*Ustaszewski et al*., 2012]. (b) Simple 3-D perspective view of plate interaction beneath Taiwan [*Lallemand et al*., 2001]. (c) Cross sections showing 1996–2012 $M \geqq 2$ background seismicity (grey circles) along profiles A-A′, indicating the configuration of the subducted Philippine Sea plate (PSP) on profile A-A′. Red circles indicate the $M \geqq 4$ guided waves events.

measure the shear wave splitting parameters. With the aid of the IASP91 global velocity model, we select 178 events that are characterized by a small incident angle at the surface (<35°) to avoid the influence of converted phases. The spatial distribution of these events in map view and cross section is shown in Figure 1. The low-frequency *S* first arrival has energy confined below 2 Hz, as shown in Figure S1 in the supporting information. Using the identified PSP-guided wave events, the seismograms are first filtered in the band 0.5–2 Hz, and then a 1–2 s time window starting from *S* arrival (~1.5 wave cycle) is selected for shear wave splitting analysis. This filter scheme provides a good signal-to-noise ratio for the *S* wave splitting analysis and avoids the high-frequency (3–10 Hz) scattering waves due to small-scale heterogeneities in the Philippine Sea slab [*Chen et al*., 2013]. Shear wave splitting analysis was carried out by both the particle motion analysis method [*Silver and Chan*, 1991] and the cross-correlation method [*Ando et al*., 1983; *Bowman and Ando*, 1987; *Kuo et al*., 1994]. This analysis employs the codes developed by *Kuo et al*. [2012], which determine the splitting parameters (fast direction φ and delay time δt) once the waveform cross correlation reaches the maximum between the waveforms in two orthogonal directions and the smallest eigenvalue of the covariance matrix reaches a minimum for the particle motion analysis [*Kuo et al*., 2012]. In this study, the shear wave splitting measurements are considered to be robust only when (1) the signal-to-noise ratio > 5; (2) the 95% confidence region is confined within ±30° for φ and within ±0.25 s for δt, as shown in Figure S2; and (3) the difference in φ and δt measurements by the two methods is small (difference in $\varphi < 5°$ and difference in $\delta t < 0.05$ s) as shown in Figure S3.

An example of the corrected fast and slow components, the particle motions, and delay time versus azimuth plot for measurements that pass these three criteria is shown in Figure S4.

With these criteria, 179 reliable shear wave splitting measurements were selected; 41 from $M \geqq 5$ events and 129 from *M*4 to *M*5 events (for spatial distribution please see Figure S5). These splitting measurements are coupled with the raypath calculated for the 3-D velocity model of *Huang et al*. [2014] and further divided into three classes of raypath. We plot the 3-D raypath in two cross sections (NE-SW and along-path directions) to ensure an in-slab path if the path is well located inside the Wadati-Benioff zone (for an example, please see Figure S6). Type I measurements have rays that travel a substantial distance in the mantle wedge, whereas for

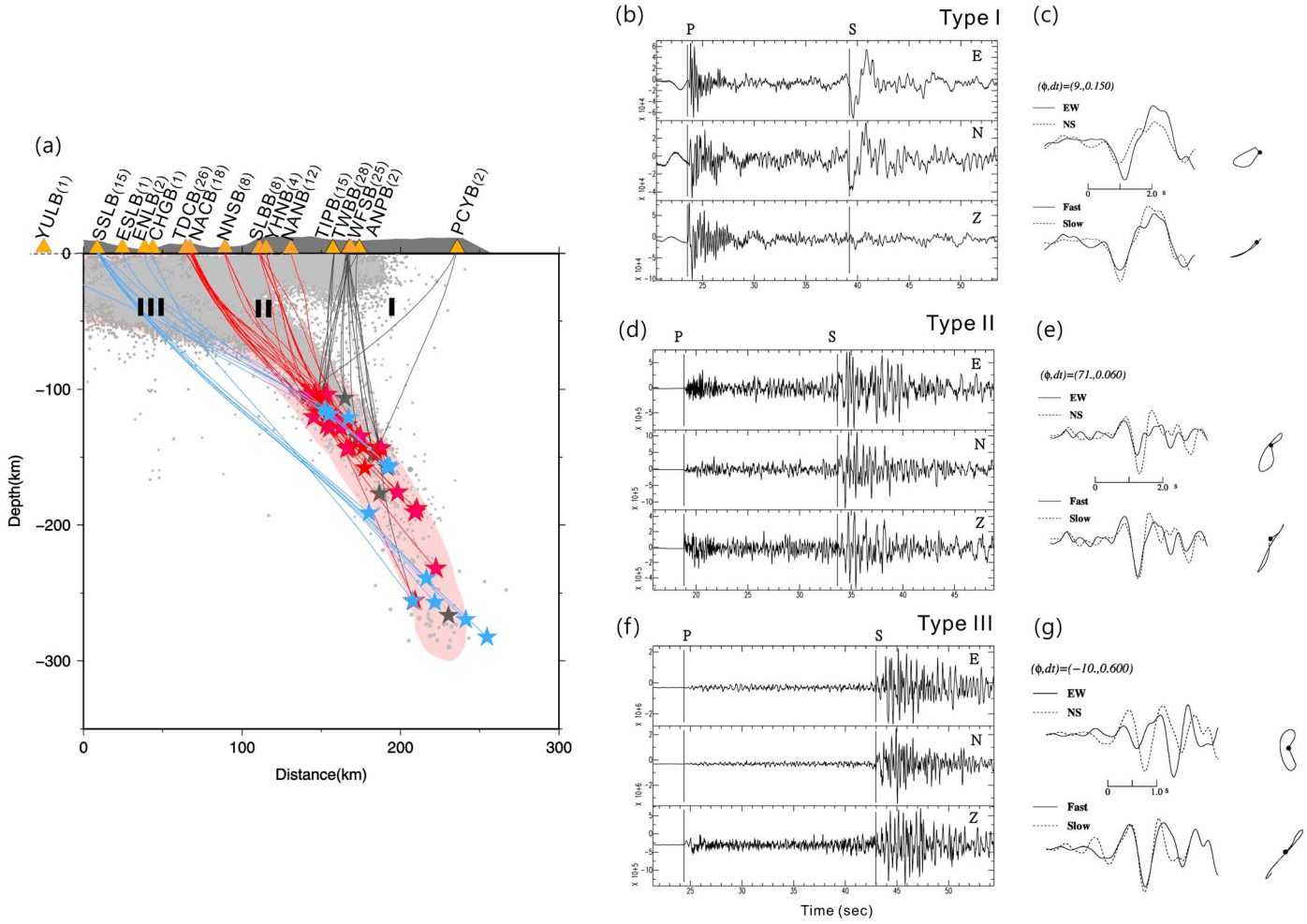

Figure 2. (a) Cross-section A-A′ in Figure 1 for seismicity (grey dots), the selected deeper than 100 km guided wave events (stars), and 3-D seismic raypath (colorful lines). Three different classes of travel path are denoted by different colors. Figure 2b shows Type I path traveling mainly in substantial distance in the mantle wedge as denoted by lines. Figure 2d shows Type II path traveling a long distance in the subducted slab as denoted by red lines in Figure 2a. Figure 2f shows Type III raypath traveling mainly through the upper mantle of the subducted slab as indicated by blue lines in Figure 2a. The number with station name represents the number of events collected. Examples showing the unfiltered seismograms and shear wave splitting measurements for (b, c) Type I, (d, e) Type II, and (f, g) Type III paths. From the left to the right are the three components seismograms and the initial and corrected particle motions. This event occurred on 15 November 2009 with magnitude 5.5 and focal depth 125 km.

Type II measurements the rays spend most time in the subducted slab. Type III measurements are dominated by passage through subslab mantle (Figure 2a). The effect of the overriding Eurasian plate is expected to be common to all raypaths. The waveform characteristics observed for Type II paths reveals relatively high frequency energy with longer duration, while Type I raypaths show lower frequency content (Figures 2b and 2d). This confirms that the Type II path travels long distances along the slab associated with the scattering due to heterogeneity in the Philippine Sea slab [*Furumura and Kennett*, 2008]. The example of splitting measurements for three type of paths is shown in Figures 2c, 2e, and 2g.

As shown in Figure 3, the shear wave splitting measurements for the three different classes of raypath (station groups) reveal distinct fast directions. Type I paths, sampling mainly fore-arc mantle, show predominant fast directions with NNE-SSW and NNW-SSE splitting at stations TWBB, TIPB, and WFSB. A roughly EW splitting is also found at stations WFSB, ANPB, and PCYB with some scatter (Figure 3b). This is consistent with shear wave splitting inferred by ocean bottom seismometer and inland BATS data by *Kuo et al*. [2012], where trench-normal mantle anisotropy is seen in the back-arc region, trench-parallel anisotropy appears near the edge of subduction, and orogen-parallel crustal anisotropy can be found farther inland. In our work, the observed NNE-SSW and NNW-SSE splitting orientation is roughly trench normal with splitting delay time of 0.09–0.46 and average of 0.24 s. A trench-parallel

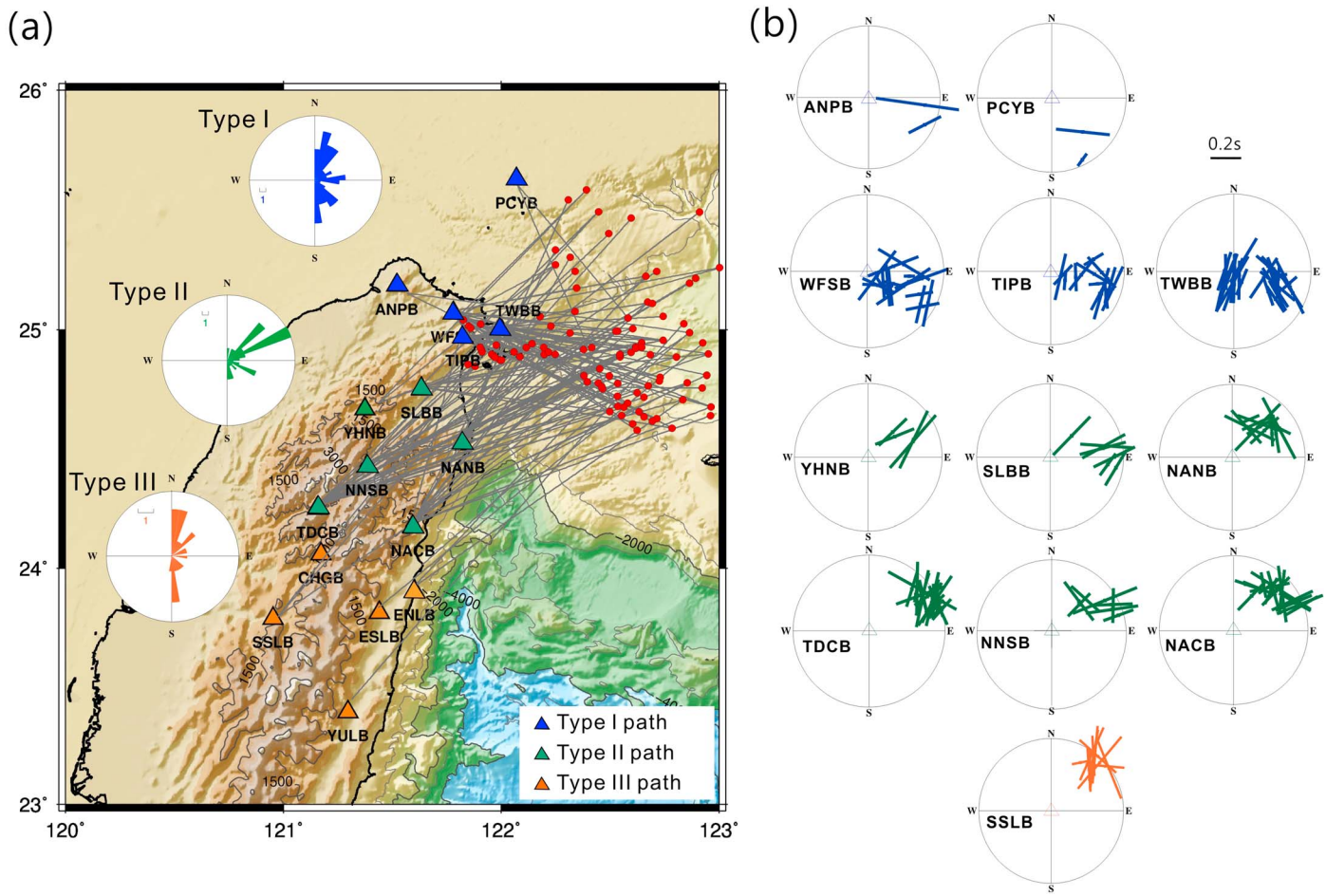

Figure 3. (a) Map view showing rose diagrams summarizing the fast direction measurements for Type I, Type II, and Type III paths. (b) Splitting parameters at each station. The stations with less than three splitting measurements are not shown (stations CHGB, ESLB, ENLB, and YULB). The orientation and length of the bar in the circle indicates the fast wave direction and delay time, respectively. The location of each bar denotes the corresponding incident angle, 0° to 35° from center to edge of the circle.

direction (EW splitting) can also be found in Type I paths, with delay time in a range from 0.06 to 0.68 s and an average of 0.25 s.

Type III raypaths show NNE fast directions that are consistent with the foliation trends in the mountain belts [*Rau et al.*, 2000; *Huang et al.*, 2006; *Chang et al.*, 2009; *Kuo-Chen et al.*, 2009]. The corresponding delay time ranges from 0.15 to 0.39 s. Note that reliable shear splitting measurements are relatively limited for Type III paths due to the longer travel distance from offshore $M > 4$ earthquakes. Here only station SSLB provides more than three splitting measurements (Figure 3b).

For Type II raypaths, the predominant fast direction is N65°E, which is commonly found at stations SLBB, YHNB,NANB, NNSB, and NACB (Figure 3b). Such a fast direction is different from the result ~N35°E inferred from *SKS* and *SKKS* waves at the same stations (subparallel to the structural trend [*Kuo-Chen et al.*, 2009]). Such a trend is also seen in our Type II observation, mainly at the TDCB station located farther inland. The various results are illustrated in the summary rose diagram in Figure 3a. The N65°E orientation is associated with delay time ranges from 0.13 to 0.45 s, which is bigger than the <0.1 s crustal anisotropy [*Tai et al.*, 2011], but smaller than the 0.6–2.6 s splitting from the upper mantle at the same stations [*Kuo-Chen et al.*, 2009]. Since the predominant fast axis for Type II paths is distinct from that for the mantle wedge and upper mantle, we argue that the orientation of N65°E from intermediate-depth events is likely to represent the anisotropy from the subducted slab near the western edge of the Ryukyu subduction zone.

The frequency dependency of shear wave splitting is not well established in this study. This is mainly because reliable measurements for high-frequency (>2 Hz) signals are only available for a limited number of events.

Most of the measurements at higher frequency show linear initial particle motion and fail to meet the criteria mentioned earlier. In the example shown in Figure S7, the difference in φ and δt is up to 30°and 0.1 s, respectively, without a consistent pattern among events at the same station. The available splitting measurements cannot therefore be regarded as reliable for frequency dependency analysis. We examined the *M*5 intermediate-depth events with more than six available stations and found that only 27% and 32% measurements for higher (2–6 Hz) and lower (0.125–0.5 Hz) frequency bands show signal-to-noise ratio higher than 5, respectively. The delay time plotted as a function of varying centroid frequency is shown in Figure S8, showing no clear frequency dependency pattern. However, there are only very limited events that produce shear wave splitting measurements in low- to high-frequency bands. Without enough consistency in the high-frequency band, we found it difficult to identify the first-order features for fast direction and delay time for both 0.125–0.5 Hz and 2–6 Hz bands. More seismic data with good signal-to-noise ratio from a longer study period and careful examination of the influence of picking error is needed for future study on the nature of frequency-dependent splitting.

3. Interpretation of N65°E Fast Direction

The Ryukyu subduction zone in southwest Japan is characterized by a trench-parallel fast direction (NE-SW) with 0.25–2.0 s splitting times in the mantle wedge [*Long and van der Hilst*, 2006], trench-parallel polarization with $<$0.2 s splitting time in the subslab mantle [*Long and van der Hilst*, 2005, 2006], and trench-parallel fast direction with ~5% anisotropy in the subducting slab using *P* wave anisotropic tomography [*Wang and Zhao*, 2012]. The observed trench-parallel splitting direction from the slab is consistent with the seafloor spreading record within the Parece Vela and Shikoku Basins of PSP at ~20 Ma [*Hall et al*., 1995; *Sdrolias et al*., 2004]. To the west, at the termination of the Ryukyu subduction zone near northern Taiwan, the strike of the trench changes to nearly E-W due to the fact that the northwestward moving PSP collides with the EP. This edge of the PSP exhibits complicated dynamics due to the subduction-collision process. In the mantle wedge, the fast directions are mostly rotated to a trench-normal (N-S) direction with 0.09–0.46 s splitting time toward the edge abutting the Eurasian lithosphere, due to the deflected flow along the arc [*Kuo et al*., 2012]. The inferred slab anisotropy, N65°E, is sufficiently distinct from the mantle wedge anisotropy to indicate different sources of anisotropy. The N65°E orientation is subparallel to the NE-SW spreading direction of PSP but slightly rotated clockwise. We argue that the slab anisotropy explored in this study may reflect the past spreading direction of the Parece Vela and Shikoku Basins with a clockwise rotation in plate motion toward the western end of the PSP. Such rotation is likely due to a horizontal compression that has been exerting on the slab by resistance of the Eurasian lithosphere against the oblique subduction of PSP, which folds the slab [*Chou et al*., 2006]. The folded geometry of PSP against Eurasian lithosphere may rotate the past spreading direction slightly. The comparison between the anisotropic structure in the oceanic lithosphere between SW Japan and NE Taiwan is shown in a conceptual model in Figure 4.

4. Responsible Anisotropic Structure

There exist two proposed classes of models for anisotropic structures in the slab: (1) Frozen-in lithospheric anisotropy due to the flow-induced alignment of olivine crystals around downgoing slabs [*Forsyth*, 1975; *Nishimura and Forsyth*, 1989]; this model predicts a fast symmetry axis orientation perpendicular to a fossil spreading ridge axis. (2) Hydration and serpentinized faulting in the shallow part of the slab due to the bending at the outer rise [*Faccenda et al*., 2008; *Healy et al*., 2009], which leads to a trench-parallel fast wave propagation. A combination of both models could be possible. However, given that anisotropy in the second model is likely to be localized in the subducting slab near the high strain area, it is relatively difficult to produce consistent anisotropic features from most of intermediate-depth earthquakes. Frozen lithospheric anisotropy in different subducting slabs appears to carry ~7% anisotropy, which is explained by the 2–6 km thick, high-velocity anisotropic mantle lid [*Song and Kim*, 2012; *Audet*, 2013]. Assuming the shear wave speed V_s is 4.7 km/s at 100 km depth, the inferred 0.13–0.45 s delay time in our work is equivalent to 3–9% anisotropy, which is not dissimilar to the value obtained from receiver functions by *Song and Kim* [2012].

In this study, shear wave splitting for the 0.5–2 Hz frequency band exhibits sensitivity to structure on the length scales of several kilometers. Type II raypaths reveal distance dependency of the observed shear wave splitting time for events deeper than 190 km, as illustrated in Figure S9. This may indicate that (1) the source

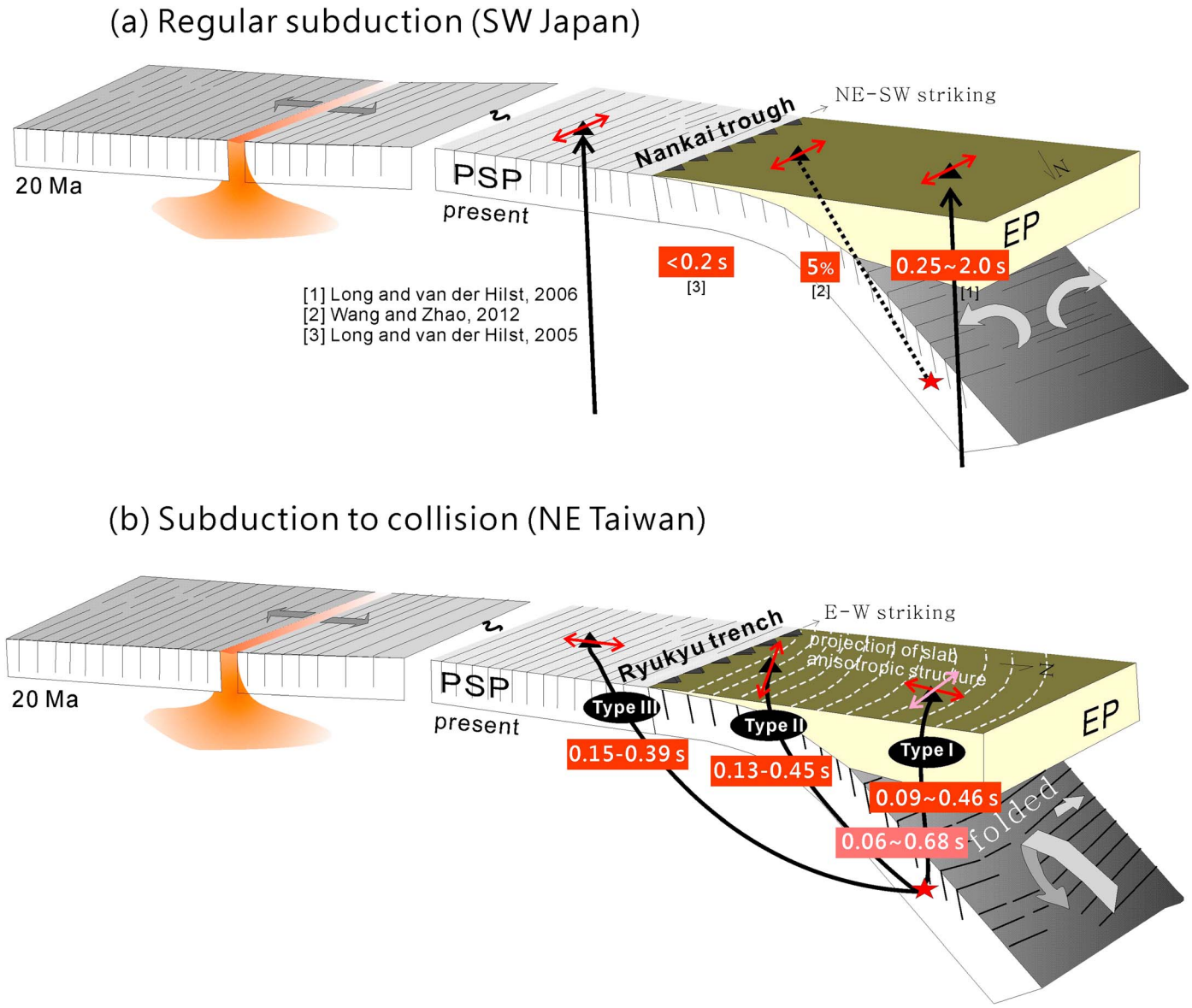

Figure 4. Conceptual model for the anisotropy observation in southwest Japan and northeast Taiwan. The thin line inside the oceanic lithosphere represents the exaggeration of frozen-in crustal anisotropic structure that is formed during lithospheric formation.

of anisotropy is not uniformly distributed over the travel distance along the slab and (2) the crustal anisotropy is not sufficient to explain such splitting time measurements. The observed splitting time is likely to be a result of different anisotropic sources from the crust, subducting slab, and mantle wedge. The influence of these combined effects might increase or decrease the shear wave splitting time with increasing source depth. However, distance-dependent effect is not commonly found for Type II raypath; the trend for events deeper than 190 km could be artificial because of very few data at the depth of 160–22 km, which requires further confirmation by more measurements.

It is also considered that quasi-laminate stochastic heterogeneity inside the plate [*Furumura and Kennett*, 2005, 2008] could provide slab-guiding behavior for high-frequency seismic waves [*Chen et al.*, 2013]. Such small-scale heterogeneities could be explained by the lamination of pyroxenite and/or chromitite layers in oceanic peridotite. Away from the ridge area, large volumes of melt infusion by the enriched pyroxenites may concentrate toward the base of the growing oceanic lithosphere [*Hirschmann*, 2010; *Shito et al.*, 2013; *Kennet and Furumura*, 2015], leading to across-plate heterogeneity. This heterogeneity develops similar sort

of traveltime anisotropy and *S* wave splitting or so-called "anisometry" [e.g., *Saito*, 2006] with a faster wave speed in the direction parallel to the lamina [see, e.g., *Backs*, 1962; *Potma*, 1995]. The way in which such anisometric structure contributes to the overall splitting measurements in the subducting slab through the increase or decrease of crystal-preferred orientation anisotropy remains an open question. Also, note that due to the multiple diffraction of seismic wave in the laminated slab, lower frequency *P* and *S* waves are developed first as precursors, while higher-frequency energy arrives later in the wave train [*Furumura and Kennett*, 2005, 2008]. The higher-frequency scattered waves may have different propagation direction for *SV* and *SH* waves, leading to a large uncertainty in splitting measurements.

The nature of anisometric structure in the slab requires further study using carefully examined higher-frequency splitting measurements coupled with numerical 3-D finite-difference method seismic wave propagation simulation where heterogeneous and anisotropic model is considered.

5. Conclusion

In northern Taiwan where the Ryukyu subduction system terminates, frequent $M \geqq 4$, intermediate-depth earthquakes provide a good tool for shear wave splitting measurements, exploiting the small incident angle at the surface for local *S* waves. In this study, we investigate anisotropy in subduction system using intermediate-depth earthquakes in the Philippine Sea slab recorded in Taiwan. The effect of slab anisotropy can be clearly separated from that in the mantle wedge and subslab effects based on the raypaths traversed in 3-D. The fast axis of shear wave splitting from the slab is N65°E with splitting time of 0.13 to 0.45 s. Such an anisotropy orientation may reflect the fossil spreading direction of PSP with a minor clockwise rotation due to the collision between PSP and EP.

Acknowledgments
We thank Ban-Yuan Kuo, Shu-Huei Hung, Wen-Tzong Liang, Cheng-Chian Liu, and Hsin-Hua Huang for sharing the codes for computing shear wave splitting parameters and 3-D seismic ray tracing. We also thank Alex Song and Ban-Yuan Kuo for helpful discussions. This work was supported by Taiwan MOST grant 103-2116-M-003-001-MY5. Seismic data are archived at the Broadband Array in Taiwan for Seismology (BATS) operated by IES.

References

Ando, M., Y. Ishikawa, and F. Yamazaki (1983), Shear wave polarization anisotropy in the upper mantle beneath Honshu, Japan, *J. Geophys. Res.*, *88*(B7), 5850–5864, doi:10.1029/JB088iB07p05850.

Audet, P. (2013), Seismic anisotropy of subducting oceanic uppermost mantle from fossil spreading, *Geophys. Res. Lett.*, *40*, 173–177, doi:10.1029/2012GL054328.

Backs, G. E. (1962), Long-wave elastic anisotropy produced by horizontal layering, *J. Geophys. Res.*, *67*, 4427–4440, doi:10.1029/JZ067i011p04427.

Bowman, J. R., and M. Ando (1987), Shear-wave splitting in the upper-mantle wedge above the Tonga subduction zone, *Geophys. J. R. Astron. Soc.*, *88*, 25–41.

Chang, E. T. Y., W. T. Liang, and Y. B. Tsai (2009), Seismic shear wave splitting in upper crust characterized by Taiwan tectonic convergence, *Geophys. J. Int.*, *177*, 1256–1264, doi:10.1111/j.1365-246X.2009.04110.x.

Chen, K. H., B. L. N. Kennett, and T. Furumura (2013), High-frequency waves guided by subducted plates underneath Taiwan and their association with seismic intensity anomalies, *J. Geophys. Res. Solid Earth*, *118*, 665–680, doi:10.1029/2012JB009691.

Chou, H. C., B. Y. Kuo, S. H. Hung, L. Y. Chiao, D. Zhao, and Y. M. Wu (2006), The Taiwan-Ryukyu subduction-collision complex: Folding of a viscoelastic slab and the double seismic zone, *J. Geophys. Res.*, *111*, B04410, doi:10.1029/2005JB003822.

Faccenda, M., L. Burlini, T. V. Gerya, and D. Mainprice (2008), Fault-induced seismic anisotropy by hydration in subducting oceanic plates, *Nature*, *455*, 1097–1100.

Forsyth, D. W. (1975), The early structural evolution and anisotropy of the oceanic upper mantle, *Geophys. J. R. Astron. Soc.*, *43*, 103–162.

Furumura, T., and B. L. N. Kennett (2005), Subduction zone guided waves and the heterogeneity structure of the subducted plate: Intensity anomalies in northern Japan, *J. Geophys. Res.*, *110*, B10302, doi:10.1029/2004JB003486.

Furumura, T., and B. L. N. Kennett (2008), A scattering waveguide in the heterogeneous subducting plate, in *Earth Heterogeneity and Scattering Effects on Seismic Waves*, *Adv. Geophys.*, vol. 50, edited by R. Dmowska, pp. 195–217, Academic Press, New York.

Hall, R., J. A. Ali, C. D. Anderson, and S. J. Baker (1995), Origin and motion history of the Philippine Sea Plate, *Tectonophysics*, *251*, 229–250.

Healy, D., S. M. Reddy, N. E. Timms, E. M. Gray, and A. V. Brovarone (2009), Trench-parallel fast axes of seismic anisotropy due to fluid-filled cracks in subducting slabs, *Earth Planet. Sci. Lett.*, *283*, 75–86, doi:10.1016/j.epsl.2009.03.0.

Hirschmann, M. M. (2010), Partial melt in the oceanic low velocity zone, *Phys. Earth Planet. Inter.*, *179*, 60–71.

Huang, B. S., W. G. Huang, W. T. Liang, R. J. Rau, and N. Hirata (2006), Anisotropy beneath an active collision orogeny of Taiwan: Results from across islands array observations, *Geophys. Res. Lett.*, *33*, L24302, doi:10.1029/2006GL027844.

Huang, H. H., Y. M. Wu, X. Song, C. H. Chang, H. Kuo-Chen, and S. J. Lee (2014), Investigating the lithospheric velocity structures beneath the Taiwan region by nonlinear joint inversion of local and teleseismic *P* wave data: Slab continuity and deflection, *Geophys. Res. Lett.*, *41*, 6350–6357, doi:10.1002/2014GL061115.

Kennet, B. L. N., and T. Furumura (2015), Toward the reconciliation of seismological and petrological perspectives on oceanic lithosphere heterogeneity, *Geochem. Geophys. Geosyst.*, *16*, 3129–3141, doi:10.1002/2015GC006017.

Kuo, B. Y., C. C. Chen, and T. C. Shin (1994), Split *S* waveforms observed in northern Taiwan: Implications for crustal anisotropy, *Geophys. Res. Lett.*, *21*(14), 1491–1494, doi:10.1029/94GL01254.

Kuo, B. Y., C. C. Wang, S. C. Lin, C. R. Lin, P. C. Chen, J. P. Jang, and H. K. Chang (2012), Shear-wave splitting at the edge of the Ryukyu subduction zone, *Earth Planet. Sci. Lett.*, *355–356*, 262–270, doi:10.1016/j.epsl.2012.08.005.

Kuo-Chen, H., F. T. Wu, D. Okaya, B. S. Huang, and W. T. Liang (2009), *SKS*/*SKKS* splitting and Taiwan orogeny, *Geophys. Res. Lett.*, *36*, L12303, doi:10.1029/2009JB038148.

Lallemand, S., Y. Font, H. Bijwaard, and H. Kao (2001), New insights on 3-D plates interaction near Taiwan from tomography and tectonic implications, *Tectonophysics*, *335*, 229–253.

Long, M. D. (2013), Constraints on subduction geodynamics from seismic anisotropy, *Rev. Geophys.*, *51*, 76–112, doi:10.1002/rog.20008.
Long, M. D., and P. G. Silver (2009), Shear wave splitting and mantle anisotropy: Measurements, interpretations, and new directions, *Surv. Geophys.*, *30*, 407–461.
Long, M. D., and R. D. van der Hilst (2005), Upper mantle anisotropy beneath Japan from shear wave splitting, *Phys. Earth Planet. Inter.*, *151*, 206–222.
Long, M. D., and R. D. van der Hilst (2006), Shear wave splitting from local events beneath the Ryukyu arc: Trench-parallel anisotropy in the mantle wedge, *Phys. Earth Planet. Inter.*, *155*, 300–312, doi:10.1016/j.pepi.2006.01.003.
Nishimura, C. E., and D. W. Forsyth (1989), The anisotropic structure in the upper mantle of the Pacific, *Geophys. J. Int.*, *96*, 203–229.
Potma, G. W. (1995), Wave propagation in stratified medium, *Geophysics*, *20*, 780–806.
Rau, R. J., W. T. Liang, H. Kao, and B. S. Huang (2000), Shear-wave anisotropy beneath the Taiwan orogeny, *Earth Planet. Sci. Lett.*, *177*, 177–192.
Saito, T. (2006), Synthesis of scalar-wave envelopes in two-dimensional weakly anisotropic random media by using the Markov approximation, *Geophys. J. Int.*, *165*, 501–515.
Sdrolias, M., W. R. Roset, and R. D. Muller (2004), An expression of Philippine Sea plate rotation: The Parece Vela and Shikoku Basins, *Tectonophysics*, *394*, 69–86.
Shito, A., D. Suetsugu, T. Furumura, H. Sugioka, and A. Ito (2013), Small-scale heterogeneities in the oceanic lithosphere inferred from guided waves, *Geophys. Res. Lett.*, *40*, 1708–1712, doi:10.1002/grl.50330.
Silver, P. G., and W. W. Chan (1991), Shear wave splitting and sub-continental mantle deformation, *J. Geophys. Res.*, *96*, 16,429–16,454, doi:10.1029/91JB00899.
Song, T. R. A., and H. Kim (2012), Anisotropic uppermost mantle in young subducted slab underplating Central Mexico, *Nat. Geosci.*, *5*, 55–59.
Tai, L. X., G. Yuan, K. F. Ma, E. T. Lee, Y. T. Shi, and H. I. Lin (2011), Crustal anisotropy in north Taiwan from shear-wave splitting, *Chin. J. Geophys.*, *54*(5), 627–636.
Ustaszewski, K., Y. M. Wu, J. Suppe, H. H. Huang, C. H. Chang, and S. Carena (2012), Crust-mantle boundaries in the Taiwan-Luzon arc-continent collision system determined from local earthquake tomography and 1D models: Implications for the mode of subduction polarity reversal, *Tectonophys. Spec. Issue: Geodyn. Environ. East Asia*, *578*, 31–49, doi:10.1016/j.tecto.2011.12.029.
Wang, J., and D. Zhao (2012), *P* wave anisotropic tomography of the Nankai subduction zone in Southwest Japan, *Geochem. Geophys. Geosyst.*, *13*, Q05017, doi:10.1029/2012GC004081.